chrome P450: Structure, Mechanism and Biochemistry, P. R. Ortiz de Montellano, Ed. (Plenum, New York, ed. 2, 1995), pp. 83–124.
4. T. L. Poulos et al., J. Biol. Chem. **260**, 16122 (1985); T. L. Poulos et al., Biochemistry **25**, 5314 (1986); T. L. Poulos and R. Raag, FASEB J. **6**, 674 (1992); H. Li et al., J. Am. Chem. Soc. **117**, 6297 (1995). Molecular replacement with the coordinates of oxidized P450cam complexed with camphor (PDB code 2CPP) as search model was used to determine the ferric P450.cam structure in a monoclinic crystal form that contains two molecules per asymmetric unit with an intermolecular K^+ ion binding site. The electron densities of the active sites of the two molecules in the asymmetric unit are not the same, but in different crystals of the same complex, corresponding molecules have similar electron densities, suggesting that the crystal lattice contacts influence the dynamics of the molecules differently. Indeed, the crystallographic environments of the two molecules differ, especially in the vicinity of the intramolecular K^+ binding site, which is connected through Tyr^{96} directly to the camphor binding site. In one molecule, this K^+ site is close to a neighboring molecule in the lattice. In general, for the experiments reported here, similar electron density features are seen in molecules 1 and 2, but mixtures seem to be present in molecule 2 that could not be modeled satisfactorily. It is possible that the two molecules represent slightly different stages of the reaction or different mixtures of species.
5. R. Raag and T. L. Poulos, Biochemistry **28**, 7585 (1989).
6. There are many examples; one is the difference between oxy- and carbonmonoxy-myoglobin. See the lively discussion in S. Borman, Chem. Eng. News **77**, 31 (1999).
7. The number of model compounds that have been synthesized and characterized is too great to permit referencing even a representative sample. For a recent review, see J. T. Groves and Y. Han, in Cytochrome P450: Structure, Mechanism and Biochemistry, P. R. Ortiz de Montellano, Ed. (Plenum, New York, ed. 2, 1995), pp. 3–48.
8. R. E. White and M. J. Coon, Annu. Rev. Biochem. **49**, 315 (1980); V. P. Miller et al., J. Biol. Chem. **267**, 8936 (1992); W. R. Patterson et al., Biochemistry **34**, 4342 (1995).
9. S. G. Sligar, J. D. Lipscomb, P. G. Debrunner, I. C. Gunsalus, Biochem. Biophys. Res. Commun. **61**, 290 (1974); C. B. Brewer and J. A. Peterson, Arch. Biochem. Biophys. **249**, 515 (1986).
10. B. L. Stoddard, Pharmacol. Ther. **70**, 215 (1996).
11. I. Schlichting and R. S. Goody, Methods Enzymol. **277**, 467 (1997).
12. D. Ringe et al., Philos. Trans. R. Soc. London Ser. A **340**, 243 (1992).
13. J. Hajdu and I. Anderson, Annu. Rev. Biophys. Biomol. Struct. **22**, 467 (1993).
14. G. A. Petsko, Philos. Trans. R. Soc. London Ser. A Math. Phys. Sci. **340**, 323 (1992).
15. J. D. Lipscomb, S. G. Sligar, M. J. Namtvedt, I. C. Gunsalus, J. Biol. Chem. **251**, 1116 (1976).
16. B. Chance, P. Angiolillo, E. K. Yang, L. Powers, FEBS Lett. **112**, 178 (1980); J. G. De Witt et al., J. Am. Chem. Soc. **113**, 9219 (1991); R. Watanabe, N. Usami, K. Kobayashi, Int. J. Radiat. Biol. **68**, 113 (1995); Y. Lindquist, W. J. Huang, G. Schneider, J. Shanklin, EMBO J. **15**, 4081 (1996); M. Erikson, A. Jordan, H. Eklund, Biochemistry **37**, 13349 (1998); E. R. Stadtman, Annu. Rev. Biochem. **62**, 797 (1993).
17. K. Kobayashi et al., Biochim. Biophys. Acta **1037**, 297 (1990); R. Davydov et al., FEBS Lett. **295**, 113 (1991).
18. M. Sharrock et al., Biochim. Biophys. Acta **420**, 8 (1976); M. J. Honeychurch, A. O. Hill, L. L. Wong, FEBS Lett. **451**, 351 (1999).
19. J. Contzen and C. Jung, Biochemistry **38**, 16253 (1999).
20. J. H. Dawson et al., J. Am. Chem. Soc. **108**, 8114 (1986); D. Harris, G. Loew, L. Waskell, J. Am. Chem. Soc. **120**, 4308 (1998).
21. V. Fülöp et al., Structure **2**, 201 (1994); S. L. Edwards, H. X. Nguyen, R. C. Hamlin, J. Kraut, Biochemistry **26**, 1503 (1987); P. Gouet et al., Nature Struct. Biol. **3**, 951 (1996).
22. J. T. Groves and G. A. McClusky, Biochem. Biophys. Res. Commun. **81**, 154 (1978); J. T. Groves and D. V. Subramanian, J. Am. Chem. Soc. **106**, 2177 (1984).
23. H. Li, S. Narasimhulu, L. M. Havran, J. D. Winkler, T. L. Poulos, J. Am. Chem. Soc. **117**, 6297 (1995).
24. I. Schlichting et al., data not shown.
25. M. Vidakovic, S. G. Sligar, H. Li, T. L. Poulos, Biochemistry **37**, 9211 (1998).
26. H. Shimada, R. Makino, M. Unno, T. Horiuchi, Y. Ishimura, in Cytochrome P450. 8th International Conference, M. C. Lechner and J. Libbey, Eds. (Eurotext, Paris, 1994), pp. 299–306.
27. N. C. Gerber and S. G. Sligar, J. Biol. Chem. **269**, 4260 (1994); J. Aikens and S. G. Sligar, J. Am. Chem. Soc. **116**, 1143 (1994); S. A. Martinis, W. M. Atkins, P. S. Stayton, S. G. Sligar, J. Am. Chem. Soc. **111**, 9252 (1989).
28. P. J. Loida and S. G. Sligar, Biochemistry **32**, 11530 (1993).
29. D. L. Harris and G. H. Loew, J. Am. Chem. Soc. **118**, 6377 (1996).
30. D. E. Benson, K. S. Suslick, S. G. Sligar, Biochemistry **36**, 5104 (1997).
31. Y. Kimata, S. Tsukada, T. Iwamoto, K. Harii, Biochem. Biophys. Res. Commun. **208**, 96 (1995).
32. R. Raag, S. A. Martinis, S. G. Sligar, T. L. Poulos, Biochemistry **30**, 11420 (1991).
33. M. Newcomb et al., J. Am. Chem. Soc. in press.
34. R. M. Esnouf, J. Mol. Graphics **15**, 133 (1997).
35. E. A. Meritt and M. E. P. Murphy, Acta Crystallogr. Sect. D **50**, 869 (1994).
36. N. C. Gerber and S. G. Sligar, J. Am. Chem. Soc. **114**, 8742 (1992).
37. T. L. Poulos, M. Perez, G. C. Wagner, J. Biol. Chem. **257**, 10427 (1982).
38. W. Kabsch, J. Appl. Crystallogr. **26**, 795 (1993).
39. J. Navaza, Acta Crystallogr. Sect. A **50**, 157 (1994).
40. A. T. Brünger, X-PLOR: A System for Crystallography and NMR, version 3.1 (Yale Univ. Press, New Haven, CT, 1992).
41. A. T. Brünger et al., Acta Crystallogr. Sect. D **54**, 905 (1998).
42. T. A. Jones, S. Cowan, J. Y. Zou, M. Kjeldgaard, Acta Crystallogr. Sect. A **47**, 110 (1991).
43. The literature of cytochrome P450 is so vast, and so many people have made important contributions, that it is impossible in the space allowed to give even a representative set of references. We have tried to cite review articles whenever possible to provide links to the original papers. We apologize to those we have been unable to include. We gratefully acknowledge G. Holtermann for designing the pressure cell; M. Davies, N. C. Gerber, E. J. Mueller, and M. Vidakovic for supplying us with protein; C. Jung, G. Rosenbaum, and K. Scheffzek for discussions; and R. S. Goody, K. C. Holmes, and W. Kabsch for continuous support and encouragement. P. Ortiz de Montellano and J. A. Peterson provided useful advice. The referees made a number of very helpful suggestions that greatly improved the manuscript. We thank the Alexander von Humboldt Stiftung, the Human Frontiers Science Project, and the Richard und Anne Liese Leyendecker Stiftung for generous support and acknowledge the European Community biotech grant BIO2-CT942060 to I.S., NIH grants GM31756 and GM33775 to S.G.S, and GM26788 to G.A.P. and D.R. Beamline X12C is supported by the U.S. Department of Energy Offices of Health and Environmental Research and of Basic Energy Sciences, NIH, and NSF. The coordinates have been submitted to the PDB: 1d26, 1d24, 1d28, and 1d29 for the ferric, reduced, oxy, and oxyferryl complex, respectively.

22 October 1999; accepted 1 February 2000

Mid-Pleistocene Acheulean-like Stone Technology of the Bose Basin, South China

Hou Yamei,[1] Richard Potts,[2*] Yuan Baoyin,[3] Guo Zhengtang,[3] Alan Deino,[4] Wang Wei,[5] Jennifer Clark,[2] Xie Guangmao,[6] Huang Weiwen[1]

Stone artifacts from the Bose basin, South China, are associated with tektites dated to 803,000 ± 3000 years ago and represent the oldest known large cutting tools (LCTs) in East Asia. Bose toolmaking is compatible with Mode 2 (Acheulean) technologies in Africa in its targeted manufacture and biased spatial distribution of LCTs, large-scale flaking, and high flake scar counts. Acheulean-like tools in the mid-Pleistocene of South China imply that Mode 2 technical advances were manifested in East Asia contemporaneously with handaxe technology in Africa and western Eurasia. Bose lithic technology is associated with a tektite airfall and forest burning.

A boundary between East Asia and western Eurasia/Africa was defined by Movius (*1*, *2*) to mark a geographic separation in early human technology and behavioral competence during most of the Pleistocene. Movius and others (*3*) observed that technologically simple methods of stone flaking persisted in China and Southeast Asia during the period when ovate large cutting tools (LCTs), specifically Acheulean bifacial handaxes and cleavers, characterized western Eurasia and Africa (currently dated at 1.6 to 0.2 million years ago). The boundary, known as the Movius Line, implies that Pleistocene East Asian populations were culturally and possibly genetically isolated (*4*), a situation that was reinforced by stable forest habitat east of the boundary (*2*, *5*). Although the Movius Line has attracted criticism (*6*–*8*), little evidence to contradict it has been presented (*9*, *10*). Analyses of Acheulean technology (*11*, *12*) have concluded that the targeted manufacture of LCTs signifies an important advance in hominin behavior (enhanced planning and technical competence) for which evidence has been lacking in the early stone technology of East Asia.

Here we describe stone tools from the

mid-Pleistocene of the Bose basin (*13*) in the Guangxi Zhuang Autonomous Region (Fig. 1) of China that provide the oldest evidence of LCT manufacture in East Asia, contemporaneous with Acheulean LCTs in western Eurasia and Africa. The basin covers ~800 km^2 and is dissected by the Youjiang River from northwest to southeast. Laterized fluvial deposits of late Pliocene and Pleistocene age crop out as seven river terraces (T1 through T7) of differing elevation associated with episodic uplift of the Qinghai-Tibetan Plateau (*14*).

Sediments of terrace 4 (T4) preserve concentrations of Paleolithic stone artifacts and dispersed tektites. The terrace, which has been fragmented by faulting, forms several platforms situated 25 to 100 m above the present river level. T4 consists of an upper sedimentary unit, 7 to 10 m thick, of poorly developed latosols underlain by reticular mottled red clay typical of laterites and of a lower unit, 5 to 20 m thick, of well-sorted cobble conglomerate. Tektites and artifacts are distributed in the upper unit within a zone 20 to 100 cm thick, which is typically 6 to 7 m above the top of the lower unit of T4. Paleolithic artifacts are abundant on the terrace surface and in three excavation localities tested between 1988 and 1996 (*15*) and have not been found in any of the other terraces.

The artifacts consist of extensively chipped cobbles of quartz, quartzite, sandstone, and chert and associated flakes (Fig. 2). Raw materials were obtainable from the basal conglomerates of T5 through T7, which were exposed during the period of artifact manufacture and deposition on the fluvial floodplain of T4 before its uplift.

The age of the stone artifacts is established by $^{40}Ar/^{39}Ar$ analyses on three suspected Australasian tektites collected in situ from two localities (two tektites from Bogu and one from Yangwu) precisely associated with the artifacts of T4 (*16, 17*). Three to four replicate, 15- to 16-step, incremental heating experiments were performed on each sample. All experiments yielded plateaus (sequences of three or more steps in which the ages could not be mutually distinguished at the 95% confidence level), usually incorporating more than 80% of the total ^{39}Ar released (*18*). Inverse isochron analysis ($^{36}Ar/^{40}Ar$ versus $^{39}Ar/^{40}Ar$) of plateau steps yielded ages concordant with plateau mean ages. The compositions of trapped argon inferred from the isochrons were within error of the atmospheric $^{40}Ar/^{39}Ar$ ratio, although there was an overall tendency toward greater-than-atmospheric ratios. Isochron ages are preferred over the straight weighted-mean calculation of ages from plateau steps because of the ability of the isochron analysis to accommodate deviations from atmospheric $^{40}Ar/^{36}Ar$ composition in the samples. Isochron ages range from 761 ± 17 to 816 ± 7 thousand years ago (ka). The best representative age is considered to be the overall weighted mean of the isochron ages from the three samples: 803 ± 3 ka (1σ). Previous $^{40}Ar/^{39}Ar$ ages of significant precision for the Australasian tektites are 783 ± 21 ka (*19*) and 784 ± 12 ka (*20*). These ages are concordant with our result, within error, and confirm the attribution of the tektites to the Australasian strewn field (*21*).

This result precisely calibrates the Bose artifacts and dates the sole period of Paleolithic toolmaking in the basin to the time of the strewn field. The age is well within the range of Acheulean assemblages of Africa and western Asia and is older than Acheulean occurrences in Europe and the elaboration of symmetry and craftsmanship in the late Acheulean (<500 ka) (*12, 22*).

The contrast between East Asian and western Eurasian/African toolmaking has been described in terms of Mode 1 (Oldowan-like, simple core/flake) versus Mode 2 (Acheulean-like, bifacial LCT) technology (*23*). Mode 1 is the oldest known type of stone flaking, well documented in excavated stone artifact samples from Beds I and II at Olduvai Gorge, Tanzania (*24–26*). Mode 2 provides the oldest evidence of targeted manufacture of large core/tool forms, such as handaxes, cleavers, knives, and picks. These LCT morphologies are typically ovate with distinctive tip ends (thin and convergent) and butt ends (thicker, sometimes unmodified). Mode 2 LCTs are made from large flakes, flat cobbles, or nodules whose properties enable thinning by percussion. Characteristics that differ from those of Mode 1 include manipulation and shaping of large rocks; production of flakes >10 cm, which were often the initial pieces on which LCTs were made; production of standardized tool forms (LCTs) that suggest the use of prescriptive procedures of percussion flaking (*9, 27*); large flake scar facets; and high flake scar counts. On a basinwide scale, moreover, Mode 2 artifacts tend to occur in a biased spatial distribution, with LCTs being abundant in delimited areas (such as paleochannels) but rare elsewhere in laterally equivalent strata (such as floodplains) (*28, 29*). This spatial bias is unknown in Mode 1.

Bose stone technology exhibits all of these Mode 2 characteristics (Table 1). The analytical sample from Bose (n = 991 specimens) is composed of excavated (84%) and surface-collected (16%) artifacts in generally very fresh condition (sharp striking platforms and flake scar intersections). The sample is characterized by the manipulation of significantly larger pieces of raw material than in

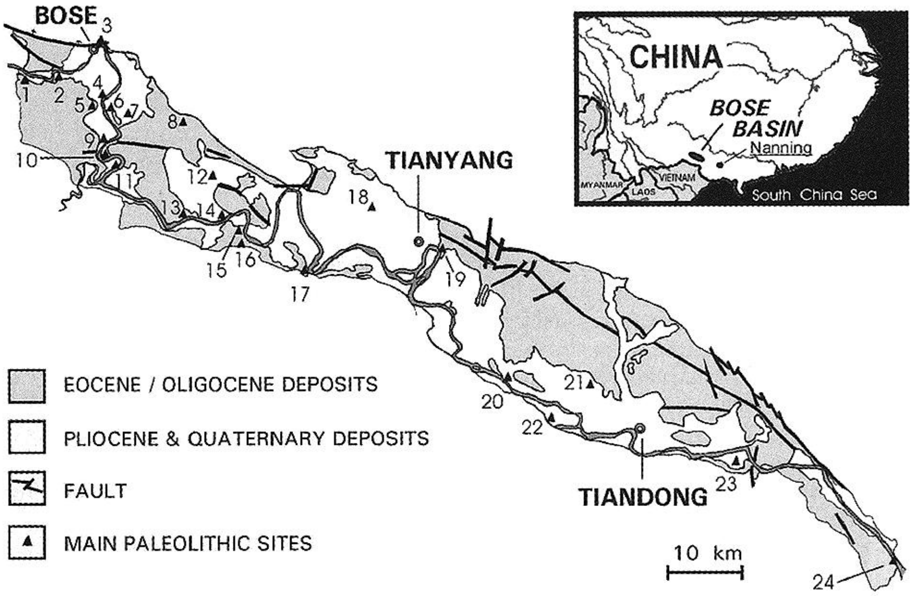

Fig. 1. Location of stone artifacts and tektites in the Bose basin. Artifact-bearing Quaternary deposits are distributed along the Youjiang River. Archeological surface and excavation sites are as follows: 1, Shangsong; 2, Dongzeng; 3, Hengshandao; 4, Dawan; 5, Shazhou; 6, Yangwu; 7, Cimu; 8, Nanposhan; 9, Jiangfeng and Datong; 10, Bogu; 11, Dafa; 12, Xiaguo; 13, Xiaomei and Nalian; 14, Damei; 15, Laikui; 16, Nayin (cave); 17, Napo; 18, Pinghepo; 19, Sanlei; 20, Xinzhou; 21, Ganlian; 22, Bodu; 23, Gaolingpo; and 24, Silin.

[1]Institute of Vertebrate Paleontology and Paleoanthropology, Chinese Academy of Sciences, Box 643, Beijing 100044, China. [2]Human Origins Program, National Museum of Natural History, Smithsonian Institution, Washington, DC 20560–0112, USA. [3]Institute of Geology and Geophysics, Chinese Academy of Sciences, Box 9825, Beijing 100029, China. [4]Berkeley Geochronology Center, 2455 Ridge Road, Berkeley, CA 94709, USA. [5]Natural History Museum of Guangxi Zhuang Autonomous Region, Nanning 530012, China. [6]History Museum of Guangxi Zhuang Autonomous Region, Nanning 530022, China.

*To whom correspondence should be addressed. E-mail: potts.rick@nmnh.si.edu

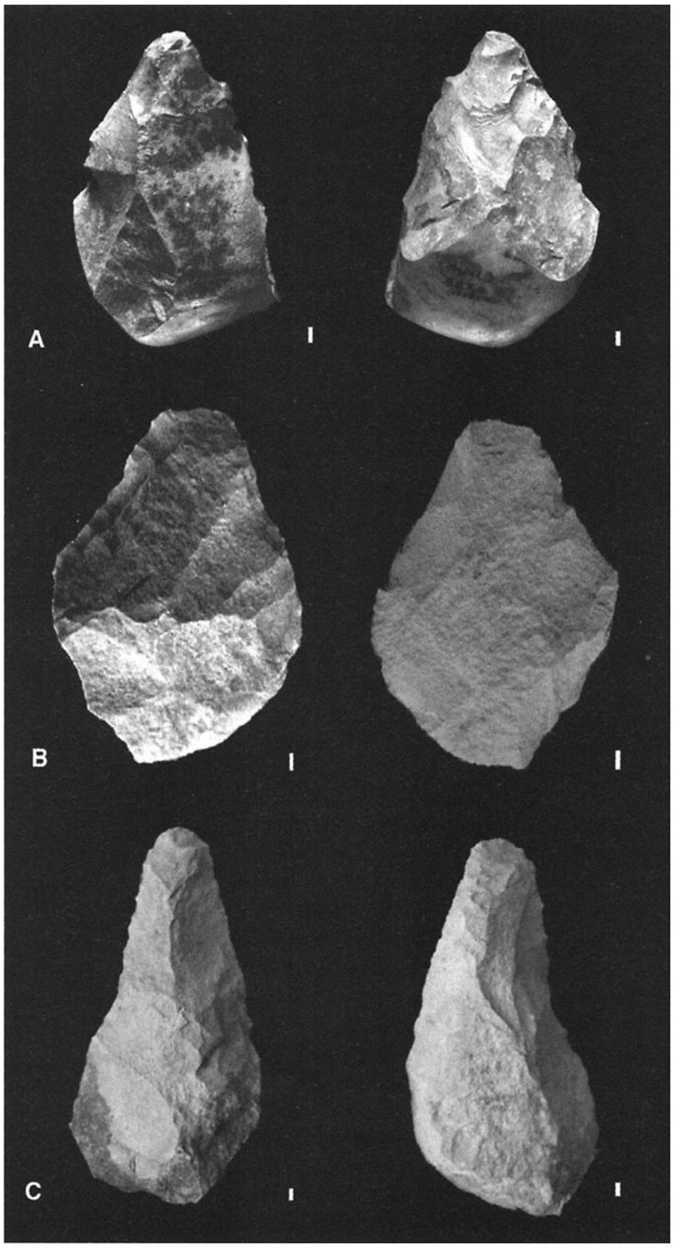

Fig. 2. Bifacial LCTs from the Bose basin. **(A)** Bogu 91001, no. 1, made on a large cobble. **(B)** Hengshandao 94, no. 3, made on a large flake with minimal retouching on the ventral surface. **(C)** Yangwu 91003, no. 1, made on a large flake. The right and left sides of the figure show opposite faces of each LCT. Scale bars at lower right of each image indicate 1 cm.

Mode 1 (*30*) and the detachment of flakes >10 cm in maximum dimension (*31*). After large flake removal, numerous smaller flakes (0.5 to 3.0 cm) were struck from either the modified cobbles or the large flakes, a combination that characterized Acheulean LCT edge shaping. Unifacial and bifacial LCTs, which possess clearly defined tip and butt ends, make up 58% of all flaked pieces (n = 172), which is well above the minimum frequency (40%) defined by Leakey (*24*) for the African Acheulean. Because of the prevalence of thick asymmetrical cobbles as an initial form (91% of all flaked pieces; 80% of LCTs) and unifacial flaking (72% of all flaked pieces; 65% of LCTs), the overall artifact sample can be distinguished from Acheulean bifacial reduction of large flakes or soft-hammer thinning (*32–34*). Nonetheless, specific artifact forms closely match those of Acheulean LCTs (Fig. 2). Although unifacial flaking dominates, a strong degree of bifacial flaking is present on 35% of LCTs in the Bose sample (Table 1, bifaciality index), nearly a quarter of which are made on large flakes and fall well within the morphological range of Acheulean handaxes, picks, or knives.

Bose LCTs represent a target morphology rather than a graded continuum with other tool forms (*35*). The number of flake scars, which increases over time in the Acheulean and is indicative of LCT refinement, is as high in the Bose LCT sample as in East African Acheulean bifaces of similar age (990 to 700 ka) from Olorgesailie, Kenya, and Beds III/IV of Olduvai, Tanzania (*36*). On the basis of extensive surface survey, there is a biased spatial distribution of unifacial and bifacial LCTs. Acheulean-like forms are delimited to the western third of the basin, whereas almost entirely unifacial forms occur in the eastern two-thirds (*37*). The area of bifacial LCTs coincides with the largest available clasts in the Bose basin, indicating that large flakes were made into bifacial LCTs where cobbles >20 cm in their maximum dimension were accessible.

Bose archeological assemblages therefore show evidence of flaking capabilities, strategies of lithic reduction, and spatial distributional patterns that are similar to those of the Acheulean. Although the tendency toward ovoid form and biconvex cross-sectional morphology that is typical of many Acheulean bifaces is rare in Bose lithic technology, prescriptive procedures were apparently applied in the selection and reduction of stone, as suggested by the concentrated thinning of LCT tips to a consistent shape, large-scale flaking of rock followed by intensive retouching, and the tendency to produce Acheulean-like bifacial forms on large flakes where raw materials of a particular size were available.

Bose stone technology is thus compatible with Mode 2 of western Eurasia/Africa just before the early-middle Pleistocene boundary. This finding implies similar technical, cultural, and cognitive capabilities on both sides of the Movius Line. The flow of population and cultural information across the line, however, may not have been extensive. The Bose basin is positioned between the Loess Plateau and South China Sea, where evidence of large environmental oscillation during the Quaternary has been documented (*38–42*). This location and the presence of poorly laterized loess at the top of the T4 section imply that Bose and South China generally were affected by significant Quaternary fluctuation. This observation implies that environmental stability did not reinforce the Movius Line throughout the Pleistocene.

One question is why stone tools are represented within a stratigraphically restricted interval in only one of the basin's fluvial terraces at about 803 ka, whereas Acheulean and other lithic traditions in western Eurasia and Africa span 10^5 to 10^6 years over numerous stratigraphic levels. One explanation is suggested by the presence of abundant charcoal and silicified wood fragments, detected during excavation and laboratory study, in precisely the same sediments containing the tektites and stone artifacts. On the basis of the co-occurrence of these remains, we suggest that the Paleolithic artifacts of Bose signal a behavioral adaptation to an episode of woody plant burning and widespread forest destruction initiated by the tektite event, which exposed cobble outcrops throughout the basin. Our findings indicate that when local or incoming populations made use of the

Table 1. Lithic artifact data from the Bose basin compared to Mode II (Acheulean) LCT assemblages and Mode I (Oldowan and Developed Oldowan) assemblages from Africa. Mean and SD (in parentheses) are given for all variables except percent made on flakes. Acheulean assemblages are from Olorgesailie Members 1 through 7 and Bed IV of Olduvai. Oldowan assemblages include DK 1-3, FLKNN-3, FLK Zinj, and FLKN-6; Developed Oldowan assemblages include HWKE-4, FLK Deinotherium, MNK Main, FCW Floor, and TK Upper (*61*). Bed IV Olduvai assemblages include PDK-IV, HEB-3, HEB-2a, HEB-2b, and WK (*33, 62, 63*). Olorgesailie data are from (*32*) and (*64*). The bifaciality index (ratio of the number of flake scars on each face) is calculated for LCTs only. n/av, no published data available; n/ap, measurement not applicable to the sample.

Site and technology	Flaked pieces	*n*	Maximum dimension (mm)	Weight (g)	Percent made on flakes	Flake scar count	Maximum flake scar length (mm)	Bifaciality index
Bose	Unifacial LCTs	64	191 (41)	1906 (1362)	6	13.1 (6.0)	93.0 (24.1)	0.03 (0.11)
	Bifacial LCTs	35	180 (32)	1534 (766)	23	24.7 (10.5)	101.7 (24.4)	0.68 (0.22)
	Non-LCTs	74	158 (78)	894 (634)	5	7.8 (4.6)	80.4 (42.3)	n/ap
	All flaked pieces	173	178 (54)	1372 (1077)	9	13.3 (9.1)	89.9 (33.5)	n/ap
Mode II	Acheulean							
Olorgesailie	LCTs	913	165 (45)	714 (407)	31	20.0 (8.2)	n/av	0.62 (0.29)
Bed IV Olduvai	LCTs	333	136 (26)	n/av	74	16.2 (6.3)	n/av	n/av
Mode I	Oldowan							
Bed I Olduvai	All flaked pieces	156	75 (16)	287 (179)	0	6.2 (2.7)	42.4 (14.6)	n/ap
	Developed Oldowan							
Bed II Olduvai	All flaked pieces	437	83 (31)	385 (395)	2	6.5 (3.5)	41.6 (16.7)	n/ap
	Bifacial LCTs	39	123 (63)	731 (747)	13	9.8 (3.4)	61.1 (33.8)	n/av

stone available in the deforested setting, their technology and related behavioral capabilities were compatible with those of the western Old World.

References and Notes

1. H. L. Movius Jr., *Trans. Am. Philos. Soc.* **38**, 330 (1949).
2. ———, in *Early Man in the Far East, Studies in Physical Anthropology*, no. 1, W. W. Howells, Ed. (Humanities Press, New York, 1969), pp. 17–77.
3. P. Teilhard de Chardin, *Early Man in China* (Institut de Géo-Biologie, Beijing, 1941).
4. Ideas advanced to explain the Movius Line include hominin migration to East Asia before the Acheulean's origin in Africa (*43*) and the loss of cultural knowledge about how to make Acheulean LCTs (*44*). Both ideas imply the isolation of toolmakers who were depauperate in the ability to produce Mode 2 LCTs after entering East Asia.
5. A stable tropical-to-subtropical setting, indicated by lateritized soils (*45*), is thought to have prompted the development in East Asia of simple lithic and nonlithic technology originally adapted to forested habitats, whereas the Acheulean developed in open savanna and Ice-Age environments of the western Old World (*46–49*).
6. S. Yi and G. A. Clark, *Curr. Anthropol.* **24**, 181 (1983).
7. V. Ranov, *Quat. Sci. Rev.* **14**, 731 (1995).
8. J. Leng, thesis, Washington University, St. Louis, MO (1992).
9. K. D. Schick, in *Integrative Paths to the Past*, R. S. Corruccini and R. L. Ciochon, Eds. (Prentice-Hall, Englewood Cliffs, NJ, 1994), pp. 569–596.
10. Previously reported East Asian sites with bifacial LCTs are dated >100 ka, but none are demonstrably older than 500 ka, including Chongokni (*50*), Dingcun (*51*), and Kamitakamori (*52*).
11. J. D. Clark, in *Integrative Paths to the Past*, R. S. Corruccini and R. L. Ciochon, Eds. (Prentice-Hall, Englewood Cliffs, NJ, 1994), pp. 451–469.
12. T. Wynn, *The Evolution of Spatial Competence* (University of Illinois Press, Urbana, IL, 1989).
13. Bose is the local Zhuang spelling of Baise (Mandarin), a name by which the basin and lithic industry are also known (*53, 54*).
14. B. Yuan *et al.*, *Acta Anthropol. Sin.* **18**, 215 (1999).
15. Excavation sites are Gaolingpo (n = 770 in situ artifacts), Bogu (n = 26), and Xiaomei (n = 36).
16. Assignment of the Bose T4 tektites to the Australasian group was suggested by a previous fission track analysis of a single tektite from Bogu (sample BG-93-18), which provided an initial age estimate of 732 ± 39 ka (*55*).
17. Analyses were done by incremental heating using a broad-beam CO_2 laser as the heating source (*56*). The tektites were splash-form in appearance, weighed 4.1 to 39.9 g, and consisted of exceedingly fresh, uniform black glass.
18. Supplementary data are available at *Science* Online at www.sciencemag.org/feature/data/1048032.shl.
19. This number was recalculated from (*57*) on the basis of new standards (*58*). The error is a 95% confidence limit.
20. J. Kunz, K. Bollinger, E. K. Jessberger, D. Storzer, in *Ages of Australasian Tektites* (Lunar and Planetary Science Conference XXVI, Lunar and Planetary Institute, Houston, TX, 1995), p. 809.
21. Investigation of Ocean Drilling Program cores 767 and 769 from marginal seas of the Indonesian archipelago (*59*) indicates that the Australasian impact event preceded the Brunhes-Matuyama geomagnetic polarity reversal by ~12,000 years. Our result of 803 ± 3 ka for the Bose tektites can be used to predict an age of 791 ka for the reversal. This value agrees with an age for the boundary of 791 ± 2 ka obtained by $^{40}Ar/^{39}Ar$ analysis of lavas (*60*), adjusted to the Fish Canyon tuff sanidine standard used here (*58*). The Bose T4 section did not yield a coherent magnetostratigraphy.
22. W. Roebroecks and T. van Kolfschoten, Eds., *The Earliest Occupation of Europe* (Univ. of Leiden Press, Leiden, Netherlands, 1995).
23. G. Clark, *World Prehistory* (Cambridge Univ. Press, London, 1969).
24. M. D. Leakey, *Olduvai Gorge*, vol. 3 (Cambridge Univ. Press, Cambridge, 1971).
25. N. Toth, *J. Archaeol. Sci.* **12**, 101 (1985).
26. R. Potts, *J. Anthropol. Res.* **47**, 153 (1991).
27. In the early Acheulean (before 500 ka), LCT shape was also influenced by initial form; minimal secondary flaking of large flakes, for example, yielded the standard thin, ovate form typical of Acheulean bifaces.
28. R. L. Hay, *Geology of the Olduvai Gorge* (Univ. of California Press, Berkeley, CA, 1976).
29. R. Potts, A. K. Behrensmeyer, P. Ditchfield, *J. Hum. Evol.* **37**, 747 (1999).
30. Bose LCTs (unifacial and bifacial) are significantly larger in mean maximum dimension than Oldowan (t = 22.56, df = 270, $P < 0.001$) and Developed Oldowan (t = 24.59, df = 551, $P < 0.001$) flaked pieces, Developed Oldowan LCTs (t = 6.94, df = 120, $P < 0.001$), and even Acheulean LCTs from Olorgesailie, Kenya (t = 4.32, df = 994, $P < 0.001$). Bose bifacial LCTs, however, do not differ significantly from Acheulean LCTs from Olorgesailie (t = 1.95, df = 946, $P > 0.05$). The mean weight of Bose LCTs is greater than that of Oldowan and Developed Oldowan flaked pieces and of African Acheulean LCTs. Bose LCTs made on large flakes fall at the upper end of the range of mean weight variation at Olorgesailie.
31. Bose LCTs made on flakes (16.4 cm, n = 12) differ little in mean maximum dimension from Acheulean LCTs from Olorgesailie (16.3 cm, n = 859). The mean length of the largest flake scar for all Bose LCTs (9.6 cm, n = 96) indicates regular manufacture of flakes ≥10 cm. The mean scar length is significantly greater than that for Oldowan flaked pieces (4.2 cm; t = 10.51, df = 216, $P < 0.001$); for Developed Oldowan flaked pieces (4.2 cm; t = 17.09, df = 337, $P < 0.001$); and for Developed Oldowan bifacial LCTs (6.1 cm; t = 4.62, df = 107, $P < 0.001$).
32. G. Ll. Isaac, *Olorgesailie* (Univ. of Chicago Press, Chicago, IL, 1977).
33. M. D. Leakey, *Olduvai Gorge*, vol. 5 (Cambridge Univ. Press, Cambridge, 1994).
34. M. Roberts and S. Parfitt, *Boxgrove: A Middle Pleistocene Hominid Site at Eartham Quarry, Boxgrove, West Sussex* (English Heritage, London, 1999).
35. The overall thickness of Bose LCTs was determined by the size and shape of the original cobble (71% of LCTs were made on cobbles) or by flake size (29% were made on large flakes). Tip morphology, however, was determined by repetitive flaking procedures that thinned one end, produced a straight edge (viewed edge-on), and aligned the axis connecting the tip to the butt with the maximum dimension of the piece (99% of LCTs). On 75% of the LCTs, tip thinning produced a central ridge 25 to 60 mm from the tip, due to the intersection of flake scars from the converging edges. On the remainder, a single flake was usually detached at the tip, removing the central ridge. LCT shape ratios (for example, thickness/width at 20% of length from the tip and thickness 20%/thickness 50% of length from the tip) all had extremely low variances (range: 0.011 to 0.033), a level that Isaac (*32*) considered indicative of modal shaping of Acheulean LCTs.
36. The mean flake scar count for Bose LCTs (17.2, n = 94 LCTs) was significantly higher than for Oldowan flaked pieces (6.2, t = 7.78, df = 265, $P < 0.001$), Developed Oldowan flaked pieces (6.5, t = 11.59, df = 470, $P < 0.001$), and Developed Oldowan bifacial LCTs (9.8, t = 4.19, df = 123, $P < 0.001$). The mean scar count for bifacial LCTs from Bose (24.7, n = 33 LCTs) was higher than for Acheulean bifacial LCTs from Olorgesailie (20.0, t = 3.17, df = 890, $P < 0.01$).
37. Ninety-one percent of the bifacial LCT sample (n = 35 specimens) was from the western third of the Bose basin (Fig. 1, sites 1 through 14).
38. T. Liu, Z. Ding, N. Rutter, *Quat. Sci. Rev.* **18**, 1205 (1999).
39. Z. Guo, T. Liu, N. Federoff, Z. An, *Chin. Sci. Bull.* **38**, 586 (1993).
40. P. Wang, *Quat. Sci.* **2**, 111 (1990).

41. K.-F. Wang, Y.-L. Zhang, H. Jian, *Chin. Sci. Bull.* **36**, 1721 (1991).
42. Z. Zhu *et al.*, *Quat. Sci.* **8**, 276 (1995).
43. C. C. Swisher Jr. *et al.*, *Science* **263**, 1118 (1994).
44. N. Toth and K. Schick, in *Tools, Language and Cognition in Human Evolution*, K. R. Gibson and T. Ingold, Eds. (Cambridge Univ. Press, Cambridge, 1992), pp. 346–362.
45. P. Teilhard de Chardin, C. C. Young, W. C. Pei, H. C. Chang, *Bull. Geol. Soc. China* **14**, 179 (1935).
46. K. Hutterer, in *Sunda and Sahul: Prehistoric Studies in Southeast Asia, Melanesia and Australia*, J. Allen, J. Golson, R. Jones, Eds. (Academic Press, New York, 1977), pp. 31–72.
47. G. G. Pope, in *The Palaeoenvironment of East Asia from the Mid-Tertiary*, J. S. Aigner, N. G. Jablonski, G. Taylor, D. Walker, P. Wang, Eds. (Centre of Asian Studies, Univ. of Hong Kong, Hong Kong, 1988), pp. 1097–1123.
48. H. Watanabe, *J. Anthropol. Archaeol.* **4**, 1 (1985).
49. J. D. Clark, *Trans. R. Soc. London Ser. B* **337**, 201 (1992).
50. K. Bai, thesis, University of California, Berkeley (1988).
51. T. Chen and S. Yuan, *Archaeometry* **30**, 59 (1988).
52. H. Kajiwara, S. Fujimura, T. Kamada, Y. Yokoyama, http://tfu-www.tfu.ac.jp/kenkyushitsu/kajiwara/KAJIWARA.html (1999).
53. W. Huang, *Quat. Res.* **28**, 237 (1989).
54. ______, J. Leng, X. Yuan, G. Xie, *Acta Anthropol. Sin.* **9**, 105 (1990).
55. S.-L. Guo, W. Huang, X.-H. Hao, B.-L. Chen, *Radiat. Meas.* **28**, 565 (1997).
56. W. Sharp and A. L. Deino, *Eos* **77**, F773 (1996).
57. G. A. Izett and J. D. Obradovich, *J. Geophys. Res.* **99**, 2925 (1992).
58. P. R. Renne *et al.*, *Chem. Geol.* **145**, 117 (1998).
59. D. A. Schneider, D. V. Kent, G. A. Mello, *Earth Planet. Sci. Lett.* **111**, 395 (1992).
60. B. S. Singer and M. S. Pringle, *Earth Planet. Sci. Lett.* **139**, 41 (1996).
61. R. Potts, unpublished data on Oldowan and Developed Oldowan sites.
62. P. Callow, in *Olduvai Gorge*, vol. 5, M. D. Leakey, Ed. (Cambridge Univ. Press, Cambridge, 1994), pp. 235–253.
63. P. R. Jones, in *Olduvai Gorge*, vol. 5, M. D. Leakey, Ed. (Cambridge Univ. Press, Cambridge, 1994), pp. 254–298.
64. M. N. Noll, thesis, University of Illinois, Urbana-Champaign (2000).

65. We thank the government of the Guangxi Zhuang Autonomous Region and the Chinese Academy of Sciences for permission to conduct the Bose basin research. Supported by funds from the Smithsonian Institution's Human Origins Program and Scholarly Studies Program, by Chinese Academy of Sciences grant SEPP 9812, by National Natural Science Foundation of China grant 49894176, and by NSF. We thank W. G. Melson and F. M. Hueber for analytical assistance, M. N. Noll for data on Olorgesailie LCTs, and A. K. Behrensmeyer and A. S. Brooks for helpful discussions.

17 December 1999; accepted 31 January 2000

REPORTS

A Global View of Martian Surface Compositions from MGS-TES

Joshua L. Bandfield,* Victoria E. Hamilton, Philip R. Christensen

Thermal Emission Spectrometer (TES) data from the Mars Global Surveyor (MGS) are used to determine compositions and distributions of martian low-albedo regions. Two surface spectral signatures are identified from low-albedo regions. Comparisons with spectra of terrestrial rock samples and deconvolution results indicate that the two compositions are a basaltic composition dominated by plagioclase feldspar and clinopyroxene and an andesitic composition dominated by plagioclase feldspar and volcanic glass. The distribution of the two compositions is split roughly along the planetary dichotomy. The basaltic composition is confined to older surfaces, and the more silicic composition is concentrated in the younger northern plains.

A major objective of the TES investigation is to determine and map the mineralogy of the martian surface in order to understand the formation and development of Mars. To understand present and past conditions on Mars, it is important to determine if the surface materials are, for example, volcanic, weathering products, or chemical precipitates. We demonstrate here that martian dark materials are volcanic and that they vary significantly across the planet. These findings can help lead to an understanding of planetary mechanisms such as the development of the martian crust, heat loss processes, bulk composition, magma differentiation, and source materials of the martian soil and dust.

Previous studies have developed the methodology for separating the surface and atmospheric components of the emission of Mars (*1*, *2*), allowing detailed analysis and interpretation of the surface composition (*3*, *4*) and atmospheric properties (*5*). The spectra of the martian surface match the spectra of rock samples and linear mixtures of minerals measured in the laboratory; there is no evidence for unusual particle size or environmental effects (*3, 4*). Atmospherically corrected TES spectra of the dark surface region of Terra Cimmeria can be matched to basalt, with a derived composition dominated by plagioclase and with lesser clinopyroxene. Analysis of TES spectra has also revealed the presence of a unique area of hematite mineralization in the equatorial Sinus Meridiani region (*4*). Here we present a global map of the petrologic and mineralogic composition of martian volcanic materials with the TES data acquired since the beginning of the MGS mapping mission (*6*).

Surface spectra were retrieved with surface atmosphere separation techniques (*1*–*3*). Two independent methods have been developed that provide nearly identical results (*7*) for the variety of surfaces presented here. The analysis presented here was performed with the deconvolution algorithm (*2*). Several surface locations were also selected for analysis with the radiative transfer algorithm (*2*) to check the consistency of the results derived from the deconvolution algorithm.

Atmospherically corrected surface emissivity spectra were analyzed with two methodologies. First, a direct comparison of martian surface spectra with laboratory thermal emission spectra of terrestrial rock samples can be used to provide a good estimate of bulk composition (*3*, *8*–*11*). However, this technique may be limited because surfaces may be mixtures of minerals that do not represent a single rock composition. In addition, it is difficult to obtain precise compositions with this technique because the number of possible realistic surface compositions is far greater than any rock library can account for.

A second, more quantitative technique is linear deconvolution of surface emissivity spectra using a spectral library of minerals (*11*–*14*). This technique takes advantage of the fact that a thermal infrared spectrum of a mixed mineral surface may be closely modeled with a linear combination of mineral spectra multiplied by their areal concentrations (*11*–*16*). Linear deconvolution of laboratory spectra may be used to retrieve the modal mineralogies of a variety of rock samples to within 5 to 10 volume % (5–10 vol. %) of optical modes (*11*, *14*). The uncertainty for the martian TES spectra is somewhat higher than these laboratory studies (~10–15 vol. %) (*3, 14*) because the martian surface spectra were acquired at lower spectral resolution, have a more limited wavelength range, and have additional uncertainties due to the removal of atmospheric effects.

Spectra of mineral mixtures, such as rocks or TES observations, are often difficult to

Department of Geology, Arizona State University, Tempe, AZ 85287–1404, USA.

*To whom correspondence should be addressed. E-mail: joshband@asu.edu